



Journal Homepage: -www.journalijar.com

INTERNATIONAL JOURNAL OF ADVANCED RESEARCH (IJAR)

Article DOI:10.21474/IJAR01/13452
DOI URL: <http://dx.doi.org/10.21474/IJAR01/13452>



RESEARCH ARTICLE

DELINEATION OF LINEAMENTS IN THE REGION OF OUADDAÏ (CHAD) USING GRAVITY DATA

Diab Ahmad Diab, Philippe Njandjock Nouck, Abdelhakim Boukar, Zakari Arétouyap, Janvier Domra Kana and Valentin Oyoa

Ecole Normale Supérieure de N'Djaména; B.P. 460 N'Djaména - Tchad.

Manuscript Info

Manuscript History

Received: 25 July 2021

Final Accepted: 29 August 2021

Published: September 2021

Key words:-

Gravity; Horizontal and Vertical Gradient; Upward Continuation; Fault; Ouaddai; Chad

Abstract

The gravity map of Ouaddai in the eastern region of Chad exhibits important anomalies that are often delimited by the high gravity gradients, resulting from the density contrasts between various anomaly sources. This presumes an important tectonic activity in zone. Because of its arid and desert nature, the region is water-poor or even lacking water resources. The main source of water in the region is made of very deep aquifers. The gravity analysis from this study helps to better understand the network of faults in the area. Many complementary approaches of the gravity data processing have been applied, namely the horizontal gradient coupled to the upward and downward continuation and the Euler method. Results from the data filtering have allowed highlighting faults network in various directions (SSW-NNE; S-N; E-W, NE-SW) and the main direction. In total, 37 major faults were detected with various lengths including 11 (F6, F9, F10, F12, F17, F29, F31, F34, F35, F37) for a cumulative total length of 353 km oriented towards Bongor basin and 15 others (F1, F4, F7, F8, F11, F13, F18, F20, F23, F25, F26, F27, F28, F30, F33), for a cumulative total length of 621 km, oriented towards Doba basin. These faults are of paramount importance with great potential impacts on the region's hydrocarbon reservoirs. These results in one hand confirmed some known faults from the previous investigations. In the other hand, the study helps to identify other new and unknown tectonic signatures.

Copy Right, IJAR, 2021.. All rights reserved.

Introduction:-

Lineaments inform on the faults network in a region. They are of utmost importance in geophysical surveys because of their numerous applications. Those applications are oriented towards various focal points including three major ones in the Ouaddai region: circulation and reservoir of groundwater, circulation and reservoir of oil and gas, and civil engineering. Many researchers, scientists and engineers used lineaments for this purpose through the world. Teikeu et al. (2016) used lineaments to analyze the hydrogeophysical activity in the Yaoundé region using remote sensing and GIS techniques; Mohammed et al. (2010) highlighted the importance of basement fracture in the attractiveness of reservoir exploration in the Sabatayn Basin, Yemen. Those subsurface lineaments extracted from seismic, magnetic and gravity data enabled to improve the oil reservoir exploration. Roure et al. (2005) noticed the incidence and the importance of tectonics and natural fluid migration on reservoir evolution in Foreland Fold-and-Thrust Belts. Per Sander et al. (1997) analysed lineaments derived from remote sensing data with respect to groundwater in the Voltaian Basin of Central Ghana.

Corresponding Author:- Diab Ahmad Diab

Address:- Ecole Normale Supérieure de N'Djaména; B.P. 460 N'Djaména - Tchad.

Chad lineaments have always interested researchers and scientists since earlier 70s. Louis (1970) interpreted the anomaly to be caused by subcrustal material that was transferred to upper crustal levels and, dated the lineaments to be older than Cretaceous. Burke and Whiteman (1973) dated the Poli triple-rift junction including the Chad anomaly and suggested that its age approximates 130–80 Ma. Fairhead and Green (1989) and Mckenzie (1978) described the Chad gravity anomaly within the context of lithospheric extension and basin formation. More recently, Liégeois et al. (2012) described the gravity anomaly as coinciding with the eastern border of a hypothetical Chad craton, a remnant of the pre-Neoproterozoic Saharan craton. Palvis et al. (2012) used a new global gravity model and satellite data to reinterpret the national lineament system. Li et al. (2013) interpreted the Chad gravity data and especially lineament, by the continuous wavelet transform, and highlighted a new exciting finding according to which Chad line delineates a first order geological boundary.

However, almost all those investigations aim at dating new geological structures. Furthermore, they are carried out at a very large scale (national). And for this, the survey is not well refined. The present study addresses the arid and desert region of Ouaddai, and aimed at highlighting new faults system, since lineament has various applications in groundwater monitoring, gas and oil exploration and exploitation, and civil engineering management. For this, gravity data are analyzed using complementary filtering method as horizontal gradients coupled to the upwards continuation. The Euler method has been used to deeply examine the lineaments network in the region.

Material and Methods:-

Data and study area

Ouaddai is located in the arid and desert eastern part of Chad. This densely populated region is experiencing a serious problem of water stress due to the inexistence of shallow groundwater sources. Hence, deeper aquifers are the only water sources in the region. Efficient and sustainable exploitation/management of these resources need enough knowledge about the region geology and especially its tectonics. To avoid useless investments in drillings and other equipment charges, it is highly advisable to conduct geophysical surveys in order to detect and accurately locate aquifers. Such investigations may also enable to better understand the underground structures, and to draw the local gravity map.

The study area is comprised between longitudes 19° - 22° E and latitudes 13° -15° N, within sahelo-sudanese climate zone (Figure 1). It can be divided into two main geological entities: the massif of Ouaddai and the recent sedimentary formation of plains. In the massif of Ouaddai, two types of rocks can be identified: the granites and the sedimentary series inside the massifs. Dominant rocks in this entity are granites from calco-alkalin and porphyriod. In some places, there are traces of gneisses and micachists. Veins of micagranites posterior to granites are visible on the surface in form of ridge orientated in three main directions S-E, N-W, S-W. These veins conceive very rough reliefs. The series of sedimentary massifs occupy a relatively important place in the massif of Ouaddai. Soils are rare or thin due to the intense erosion activities. The recent sedimentary formations largely dominate the west massifs of Ouaddai where the granites are seldom forming the iceberg merged in the sediments. The substratum made of granites and gneiss is shallower and extends over large distance on the surface.

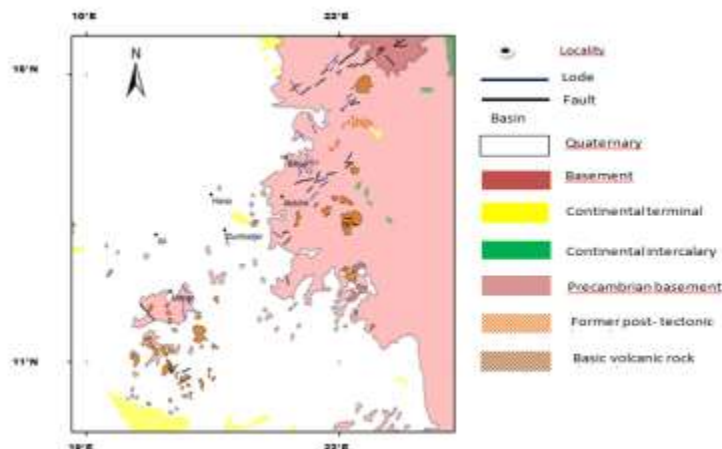


Figure 1:- Map of the surface geology with various formations along with Ouaddai.

Data used in this study have been collected during the campaign conducted by ORSTOM in 1968. These data are very sparse, with an irregular distribution as shown in Figure 2. For this, geostatistical kriging method is used to interpolate and densify the dataset. This interpolation technique is based on the variogram (Pohlmann, 1993). This method has been used to draw the map of the Bouguer anomaly, represented in Figure 3 (Diab et al., 2013). This map shows a series of anomalies with values ranged from -60mGal to -50 mGal in Oumhadjer, from -75mGal to -70mGal in Abeche, and from -80mGal to -70 mGal in Biltine.

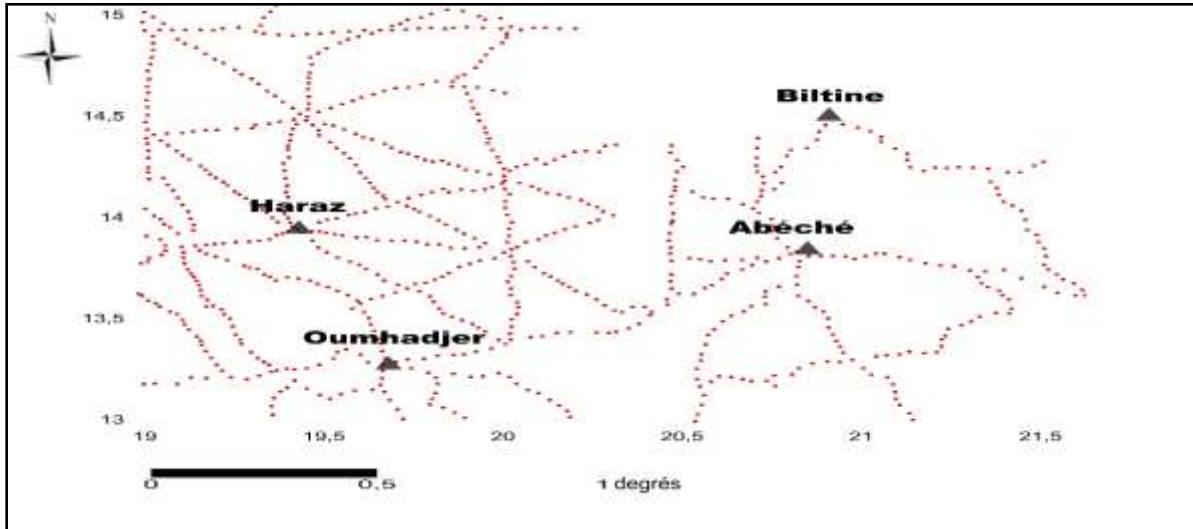


Figure 2:- Spatial distribution of gravity data within the study area.

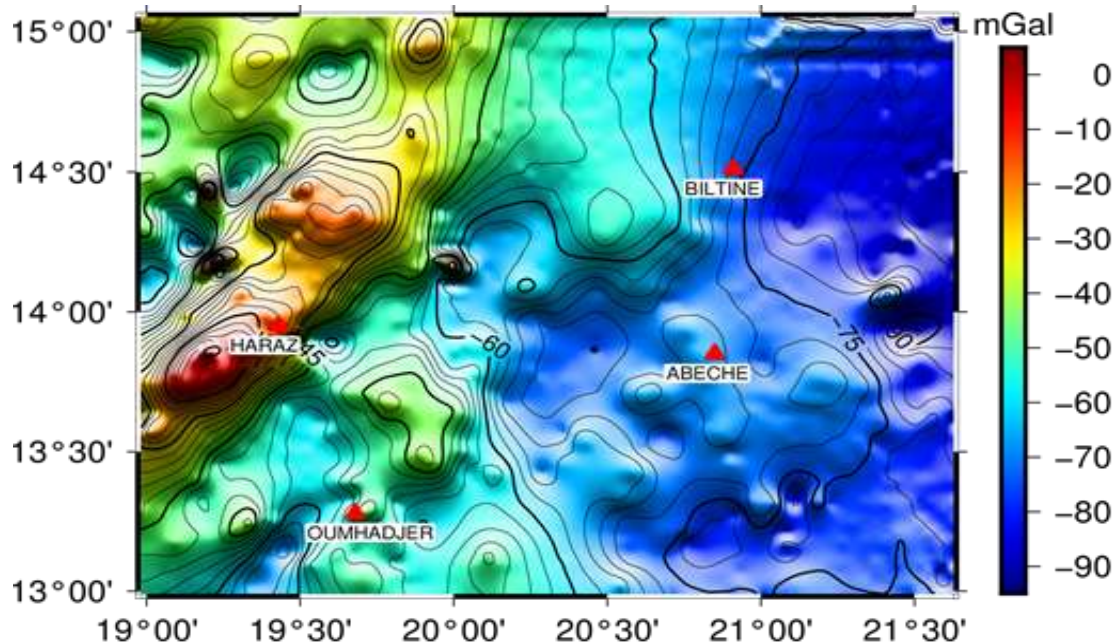


Figure 3:- Map of Bouguer anomaly.

Methods used

In this study, three methods of data processing have been used to determine the faults, their dips, lateral extension and depths. The vertical and horizontal gradients coupled to the upward continuation and the Euler's deconvolution have also been applied.

The vertical gradient enabled, in the absence of sedimentary heterogeneity, to recognize the shallower and deeper part of the bedrock. The interest in converting the map of vertical gradient field of gravity (that is the first derivative) has been evidenced long time ago (Eyjen, 1936; Baranov, 1957; Le Mou  l, 1970; G  rard and Griveau, 1972; Galdeano, 1980). To highlight the shallower lithology, it is necessary to perform a new transformation of the anomaly map. This transformation will vanish the regional component that hides the relationship between the geology of the shallow bedrock and the form of anomalies, using formula $(\partial g/\partial z)$. This transformation vanishes the regional component that sometime deforms or hides the relation between the geology of the shallower bedrock and the form of anomaly. It is then important insofar it shows the areas where the bedrock is shallower or deeper and, moreover, the tectonic accidents with small extension. This component is expressed by equation 1.

$$g_z = \frac{\partial g}{\partial z} \quad (1)$$

This transformation operates as an amplifier for high frequencies, concerning anomalies of small extension, or in at least one direction. It highlights the areas of deep bedrock and the tectonic accidents that extend over large distances.

The horizontal gradient coupled to the upward continuation enables to localize faults and determine their dips (Archibald and Bochetti, 1999; Khattach et al., 2006; Vani   et al., 2005; 2006). The circular contacts are limited by intrusive bodies.

Blakely and Simpson (1986) have proposed a method to automatically determine gradient maxima, from a grid of values presented on a 3x3 window. The application of this method to a gravity map shows that the maxima of horizontal gradient form the ripple on the top of abrupt change of densities. The positions of the point of inflexion are easily determined by the localization of the modulus of the total horizontal gradient as shown by equation 2.

$$g_h = \left[\left(\frac{\partial g}{\partial x} \right)^2 + \left(\frac{\partial g}{\partial y} \right)^2 \right]^{1/2} \quad (2)$$

To determine the orientation of the dip of the various contacts, upward continuations of the Bouguer anomaly have been performed at different altitude. For each level, the maxima of horizontal gradient have been determined. In practice, the highest upward continuations correspond to the deepest contact and vice-versa. If the structures are vertical, all the maxima will be superposed, therefore, the upwards displacement of the maxima indicates the orientation of the dip.

The Euler's deconvolution allows to localize the horizontal contacts and also estimate the depth (Keating, 1998; AsfiraneHaddadji and Galdeano, 2000). This method is based on a mathematical procedure represented by the Euler's homogeneity equation 3 (Thompson, 1982).

$$f(tx, ty, tz) = t^n f(x, y, z) \quad (3)$$

Thompson (1982) has developed a method based on the properties functions of the potential field. He noticed that these functions are in agreement with the Euler equation of homogeneity. Read et al. (1990) have generalized these techniques in the case of maps and then, the method allows to accurately localize the anomalies sources in a horizontal surface and determine also their depths. The Euler's equation can be written in the following form (equation 4):

$$(x - x_0) \frac{\partial g}{\partial x} + (y - y_0) \frac{\partial g}{\partial y} + (z - z_0) \frac{\partial g}{\partial z} = -NT(x, y) \quad (4)$$

Where (x_0, y_0, z_0) are the coordinates of the gravity source, g is the field intensity measured at the point (x, y, z) , N indicates the structure's index and stands for the source geometry.

Thompson (1982) and Read et al. (1990) have proved that the structural index is very important and established a structural index N for a certain number of structures. The structural index can take values ranged between 0 and 3

corresponding to the entire number for some simple structures. These authors considered that $N = 1$ is the most adapted index for the thin veins, dykes and faults with feeble vertical turning down. The index $N = 0$ is amenable for faults with bigger turning down and $N = 0.5$ for the transitional. The efficiency of this method has been confirmed by several investigations (Archibald and Bochetti, 1999; Everaerts and Mansy, 2001; Khattach et al., 2004; Vanié et al., 2005; Chennouf et al., 2007; El Gout et al., 2010).

Results and Discussion:-

Map of the vertical gradient

The map of the vertical gradient of the region is represented by Figure 4. This map highlights the area of positive gradients that can easily be distinguished from the zones of negative gradient. It illustrates the lateral separation of the anomalies with an amplification of the gravity of the superficial density contrast to the detriment of the deep density contrasts. The anomalies of the Haraz are characterized by a vertical gradient of positive values can reach 1.26 mGal/Km. In the western part of this region, the values reached -1.55 mGal/Km. This confirms a raise of heavy that can be seen on the map of the Bouguer anomaly. Also, in the Ouaddai region, the gradients of anomaly are positive, involving that the area is not in a sedimentary basin on the contrary to what can be deduced from the map of the Bouguer anomalies. There is a density contrast within the bedrock. In the western part of the region, the anomaly gradients reach -1.55 mGal/Km. Biltine area is marked by negative gradients, whereas the Oumhadjer town is characterized by positive gradients of about 1.26 mGal/ Km, and negative gradients of about -1.55 mGal/ Km in its western part.

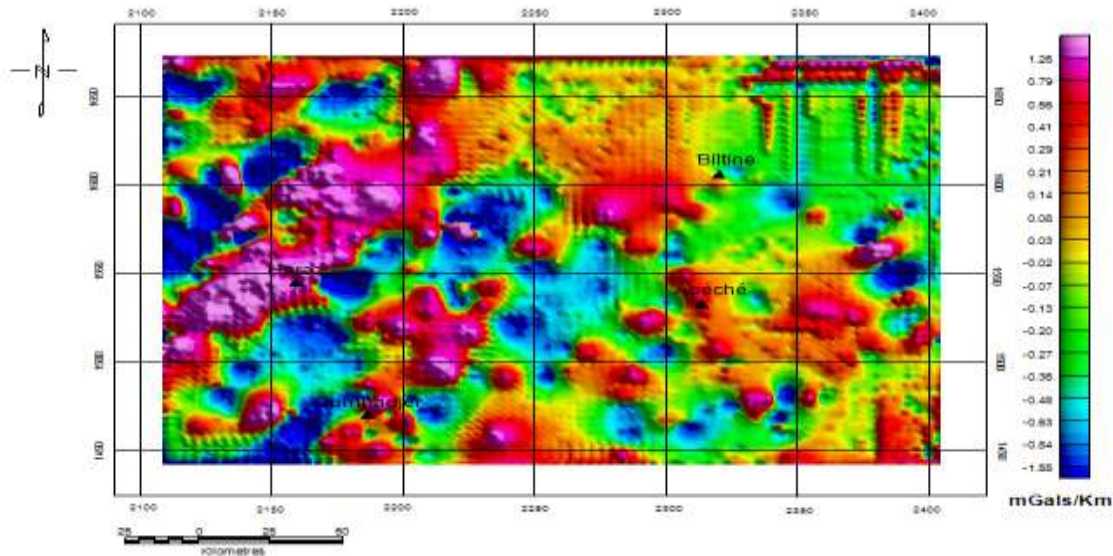


Figure 4:- Map of the vertical gradient.

Horizontal gradient coupled to the upward continuation

The total horizontal derivative of the Bouguer anomalies has been computed using equation (2), and shown in Figure 5. It reveals the amplitude of the horizontal gradient with various forms, mostly orientated on the NE-SW direction concentrated westward.

From the map, there are zones of gradients corresponding to contacts or faults (e.g. the axis passing through Haraz with NE-SW direction and the axis passing through Oumhadjer). Others correspond to the presence of the intrusive structures in the eastern part of the study area, namely Oumhadjer and Abéché vicinity.

To localize contacts and their orientations, we used a 4 km-lag of upwards continuation of the Bouguer anomaly in series of altitudes up to 20 Km. At each high, the maxima of the anomaly gradient have been localized. The maxima determined from the map of Bouguer anomaly and the upward continuation have been superposed as shown in Figure 6. The superposition is also done with the horizontal gradient of Bouguer anomalies (Figure 7).

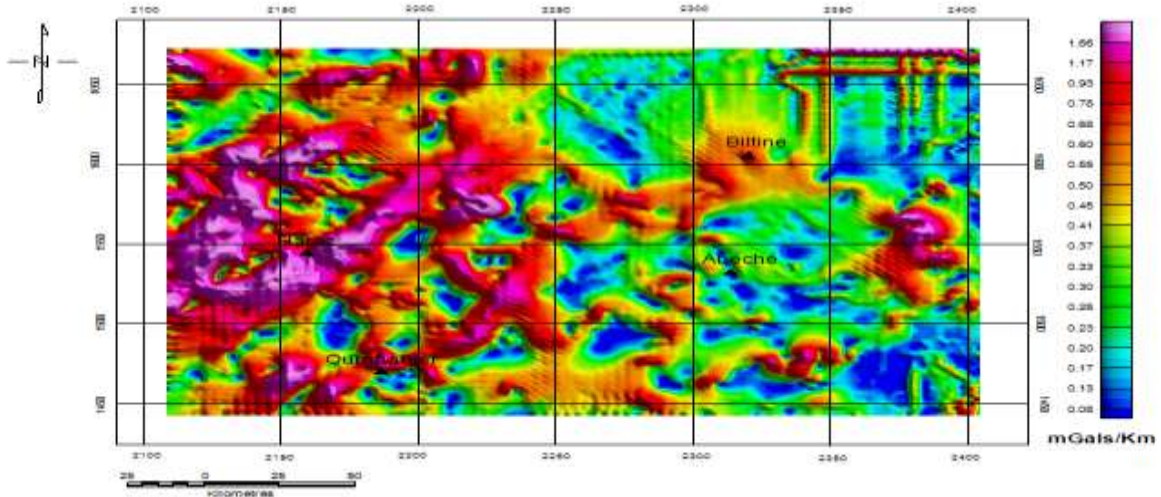


Figure 5:- Map of the horizontal gradient.

The digitalization of the contacts interpreted as faults (Figure 9) and their orientation reveals the presence of faults network.

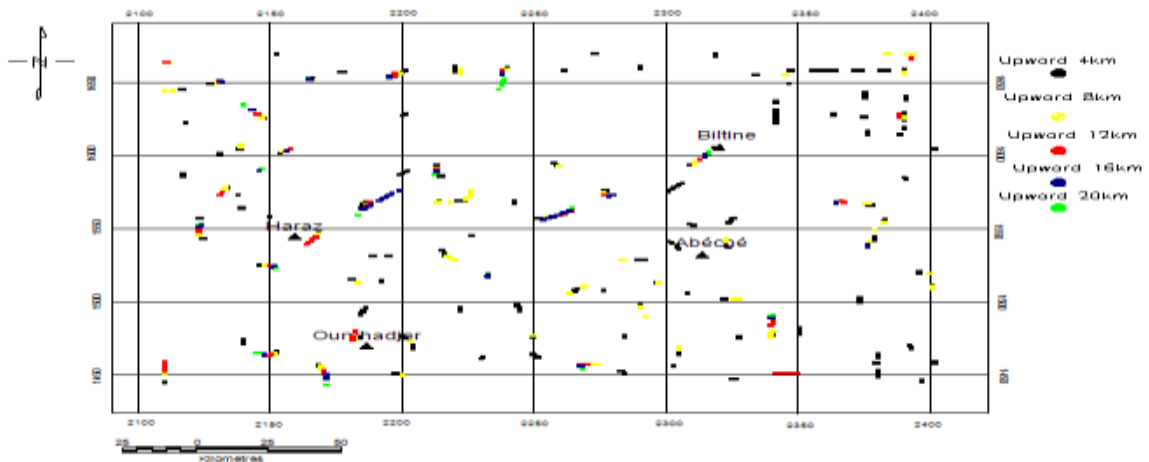


Figure 6:- Map of the superposition of the maxima.

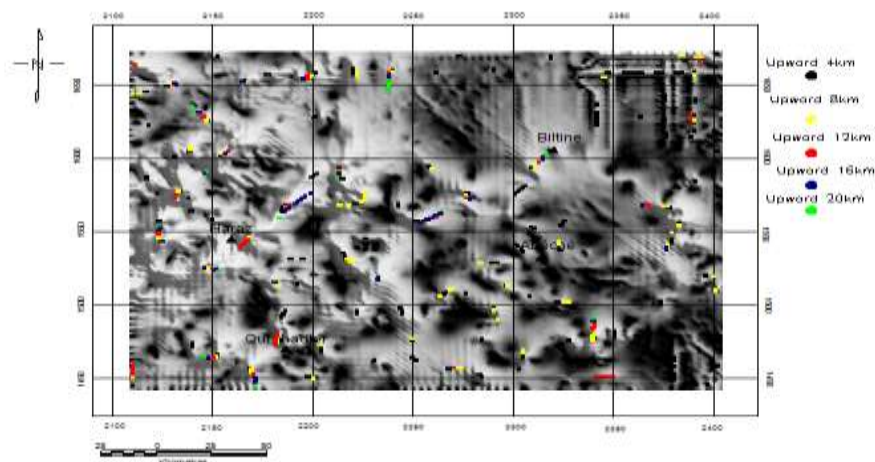


Figure 7:- Superposition of the maxima of points on the Map of Bouguer anomaly gradient.

Contribution of the deconvolution

The Euler's solution for the structural index $N = 0$ are presented in Figure 8. Their alignments reveal other faults, moreover, apart from the main contacts deduced from different gravity filtering methods (gradient coupled to the upward continuation). The deeper accidents are mostly oriented SSO-NNE and S-N and, with a depth up to 13.35 Km. There are other family of faults from directions E-O and SSE-SNE. They are shallower faults with depths rarely reaching 1 Km.

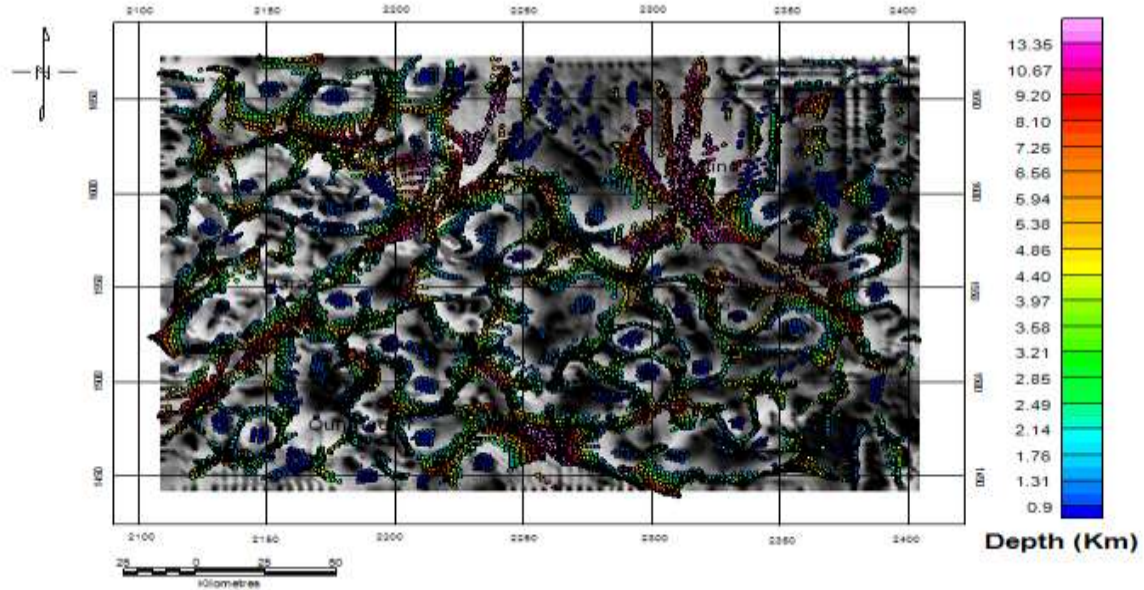


Figure 8:- Map of the Euler's solution for the structural indice $IS=0$, a window of 10×10 with a maximum relative error of about 15% on the map of the horizontal gradient of the Bouguer anomaly.

Structural map (Gravity lineaments)

A combination of the method of horizontal gradient coupled to the upward continuation and the Euler's deconvolution led to perform maps of gravity lineaments. The superposition of these maps reveals important complementary results in the deduced faults system. Hence, four families of faults have been evidenced within SSO-NNE, S-N, E-O and SSE-SNE directions (Figure 9). These informations are in a good agreement with previous geophysical findings (Louis 1970). They also enabled to highlight several shallow and deep tectonic accidents that have been up to now unidentified.

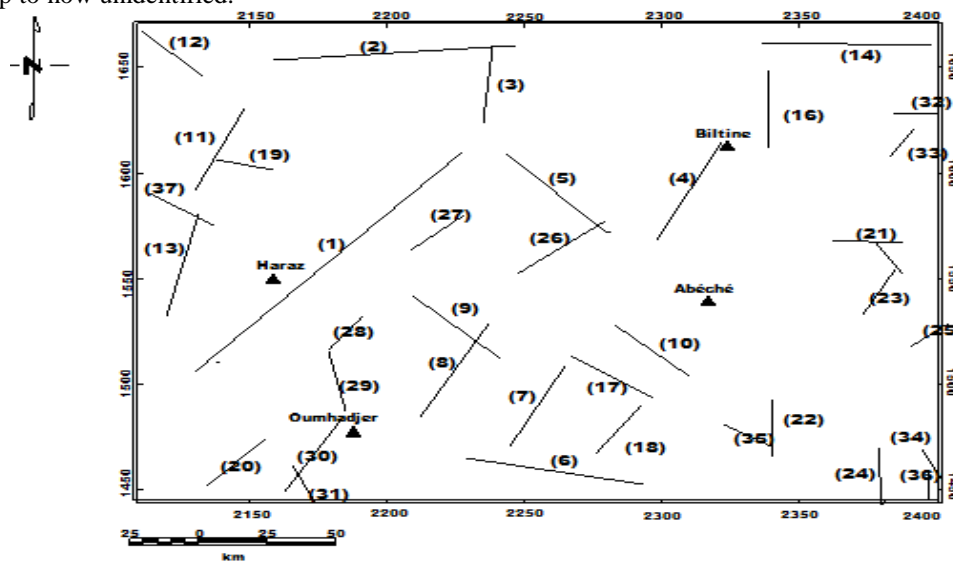


Figure 9 :-Map of major gravity lineaments.

Tableau 1:- Direction of different gravity lineaments.

Orientation	Fault number	Orientation	Fault Number
N42°E	1	N130°E	10
N27°E	4	N135°E	12
N27°E	7	N123°E	17
N29°E	8	N167°E	29
N24°E	11	N154°E	31
N12°E	13	N153°E	34
N34°E	18	N121°E	35
N45°E	20	N124°E	37
N30°E	23	N90°E	2
N51°E	25	N90°E	14
N51°E	26	N90°E	19
N45°E	27	N90°E	21
N38°E	28	N90°E	32
N29°E	30	N0°E	3
N31°E	33	N0°E	16
N135°E	5	N0°E	22
N101°E	6	N0°E	24
N134°E	9	N0°E	36

Thirty seven major faults, shown in Table 2, were identified in the region. Their lengths range from 13.37 km (F36) to 142.46 km (F1) with an average of 43.57 km and a standard deviation of 23.81 km. Eight among them have a length less than 20 km. Sixteen have a length value between 20 and 40 km, 7 have a length ranged from 41 km to 60 km, and 4 have a length greater than 60 km. These faults are of paramount importance with great potential impact on the region's hydrocarbon reservoirs. Indeed, 11 faults (F5, F6, F9, F10, F12, F17, F29, F31, F34, F35, F37) for a cumulative total length of 353 km are oriented towards Bongor basin and 15 others (F1, F4, F7, F8, F11, F13, F18, F20, F23, F25, F26, F27, F28, F30, F33), for a cumulative total length of 621 km, are oriented towards Doba basin.

Table 2:- Thirty seven faults detected in the region with their sizes.

Faults	Length (km)	Faults	Length (km)	Faults	Length (km)
F36	13.37	F21	25.05	F26	41.42
F34	13.67	F27	26.08	F11	42.06
F33	15.09	F37	26.35	F7	42.91
F32	15.75	F29	27.54	F9	43.52
F15	16.70	F18	27.58	F13	49.18
F25	17.08	F12	30.04	F8	50.65
F31	18.36	F20	31.39	F5	51.28
F35	19.00	F3	35.47	F4	51.42
F28	20.52	F17	35.60	F14	60.58
F19	20.96	F16	35.78	F6	64.18
F22	24.35	F10	36.17	F2	87.56
F23	24.56	F30	38.28	F1	142.46
F24	24.81				

Conclusion:-

The combination of the results from different methods of interpretation namely the horizontal gradient coupled to the upward continuation and the Euler deconvolution of the Bouguer anomaly of the Ouaddai area led to the elaboration of the map of gravity lineaments. The statistical analysis of the results enabled to highlight four regional series of gravimetric lineaments within SSO-NNE, SN, EO and SSE-SNE directions. The Euler's method revealed other lineaments that have not been identified using other filtering techniques (the horizontal gradient coupled to upward continuation) and furthermore, helped to assess the depths of those lineaments. In total, 37 major faults were detected with various lengths including 11 (F5, F6, F9, F10, F12, F17, F29, F31, F34, F35, F37) for a cumulative total length of 353 km oriented towards Bongor basin and 15 others (F1, F4, F7, F8, F11, F13, F18, F20, F23, F25,

F26, F27, F28, F30, F33), for a cumulative total length of 621 km, oriented towards Doba basin. The lineaments within SSO-NNE and S-N are the deepest ones with depth of about 13.4 Km whereas those within E-O and SSE-SNE directions are shallower with depth less than 2 Km. This leads to the hypothesis of their recent formation. Several lineaments correspond to the faults known and identified by Louis et al. (1970) such as faults N° 1, 4, 7, 18, 21, 23 and 33 or supposed to exist by other structural studies. This lineaments map is of utmost importance. Indeed, it may constitute a guide for future geophysical surveys in this study area. It is also a very important tool for groundwater resources exploration and for natural risks and hazards resilience and management in the region.

References:-

1. Asfirane-Haddadji, F., Galdeano, A., 2000. L'utilisation de la déconvolution d'Euler et du signal analytique pour la localisation des sources magnétiques. *Bull Soc Géol Fr* 1: 71-81.
2. Archibald, N., Bochetti, F., 1999. Multiscale edge analysis of potential field data. *Explor Geophys* 30: 38-44.
3. Aynard, C., 1953. An attempt to interpret the gravimetric map of the northern part of the Moroccan basin of Ghareb. *Maps of the residual anomaly and first vertical derivative. GeophysPros* 1: 279-289.
4. Baranov, V., 1957. A new method for interpretation of aeromagnetic maps: Pseudogravimetric anomalies. *Geophysics* 22: 359-38.
5. Diab, A.D., Njandjock Nouck, P., Nouayou R., Oyoa V., Mahamat A.M., Manguelle-Dicoum, E., 2013. Correlation Between Gravity and Near Surface Geological Structures in Chad Republic Region. *European Journal of Scientific Research* 110: 586-594.
6. Everaerts, M., Mansy, J.L., 2001. Le filtrage des anomalies gravimétriques ; une clé pour la compréhension des structures tectoniques du Boulonnais et de l'Artois. *Bull Soc Géol Fr* 3: 267-274.
7. Evjen, H.M., 1936. The place of the vertical gradient in gravitational interpretations. *Geophysics* 1 : 127-136.
8. Galdeano, A., 1980. La cartographie aéromagnétique du Sud-Ouest de l'Europe et de la région Afar: réalisation, méthodes de traitement, applications géodynamiques. *Dissertation, Université Paris VII.*
9. Khattach, D., Keating, P., Mili, E.M., Chennouf, T., Andrieux, P., Milhi, A., 2004. Apport de la gravimétrie à l'étude de la structure du bassin des Triffa Maroc nord-oriental. : implications hydrogéologiques. *Geoscience* 336: 1427-1432.
10. Keating, B.P., 1998. Weighted Euler deconvolution of gravity data. *Geophysics* 63: 1595-1603.
11. Li, Y., Braitenberg, C., Yang, Y., 2013. Interpretation of gravity data by the continuous wavelet transform: The case of the Chad lineament. *Journal of Applied Geophysics* 90: 62-70.
12. Louis, P. 1970. Contribution de la géophysique à la connaissance géologique du bassin du Lac Tchad. *Mémoire ORSTOM.*
13. Le Mouél, J.L., 1970. Le levé aéromagnétique de la France. Calcul des composantes du champ à partir des mesures de l'intensité. *Ann Geophys* 26: 299-258.
14. Mohammed, A., Palanivel, K., Kumanan, C.J., Ramasamy, S.M., 2010. Significance of Surface Lineaments for Gas and Oil Exploration in Part of Sabatayn Basin-Yemen. *Journal of Geography and Geology* 21.: 119-128.
15. Per Sander, Minor, T.B., Chesly, M.M., 1997. Ground-water exploration based on lineament analysis and reproductibility tests. *Ground Water* 35 5.: 888-894.
16. Roure, F., Swennen, R., Schneider, F., Faure, J.L., Ferket, H., Guilhaumou, N., Osadetz, K., Robion, P., Vandeginste, V., 2005. Incidence and importance of tectonics and natural fluid migration on reservoir evolution in Foreland Fold-and-Thrust Belts. *Oil & Gas Science and Technology* 60 1.: 67-106.
17. Teikeu Assatse, W., Njandjock Nouck, P., Tabod, C.T., Akame, J.M., Nshagali Biringanin, G., 2016. Hydrogeological activity of lineaments in Yaounde Cameroon region using remote sensing and GIS techniques. *The Egyptian Journal of Remote Sensing and Space Sciences*. doi: 10.1016/j.ejrs.2015.12.006
18. Thompson, D.T., 1982. EULDPH: A new technique for making computer-assisted depth estimates from magnetic data. *Geophysics* 47 : 31-37.
19. Vanié, L.T.A., Khattach, D., Houari, M.R., 2005. Apport des filtrages des anomalies gravimétriques à l'étude des structures profondes du Maroc oriental. *Bulletin de l'Institut Scientifique, Rabat, section Sciences de la Terre* 27 : 29-40.
20. Vanié, L.T.A., Khattach, D., Houari, M.R., Chourak, M., Corchete, V., 2006. Apport des filtrages des anomalies gravimétriques dans la détermination des accidents tectoniques majeurs de l'Anti-Atlas Maroc., *Actes du 3ème Colloque Maghrébin de Géophysique Appliquée. Oujda* 11-13 mai 2006, 23-3.